

MODELING STUDY BASED ON SURFACE MOBILITY MECHANISM (GALVELE MODEL) APPLIED TO BRAZILIAN SLOW STRAIN RATE TESTS OF INCONEL ALLOY 600¹

Omar Fernandes Aly²
Miguel Mattar Neto³
Mônica Schwartzman⁴

Abstract

The stress corrosion cracking initiation and propagation are very complex processes, one type of environmentally assisted cracking, besides corrosion fatigue and hydrogen embrittlement, depending on several parameters which are classified in microstructural, mechanical and environmental. Because this complexity, there are various models which can quantify this kind of failure. For stainless steel and nickel alloys in light water nuclear reactors at high temperature, there are several mechanisms which allow to express mathematically the stress corrosion cracking initiation and propagation kinetic processes: the Rice's creep model, the slip-step dissolution and film rupture model of Ford and Andresen, the internal oxidation mechanism of Scott and Le Calvar, the enhanced surface mobility mechanism of Galvele, the numerical model of Rebak and Smialowska, hydrogen induced cracking models of Shen and Shewmon, Magnin and others. The model based on enhanced surface mobility mechanism, developed by José Galvele in Argentina, is one of the main ones which quantify the crack propagation rate of stress corrosion cracking in alloys recovered with low melting point films and with cations such as Ag⁺ (Ag-Cd Alloys) and Cu²⁺ (brass). It is also adequate for nickel superalloy Inconel 600. In this paper it is showed the results of the surface mobility model applied on Alloy 600 specimens tested by slow strain rate test equipment in CDTN laboratory in Brazil.

Key words: Inconel alloy 600; Slow strain rate test; Stress corrosion; Surface mobility model.

ESTUDO DE MODELAGEM BASEADO NO MECANISMO DE MOBILIDADE SUPERFICIAL (MODELO DE GALVELE) APLICADO A ENSAIOS NO BRASIL DE TAXA DE DEFORMAÇÃO LENTA DE LIGA INCONEL 600

Resumo

A iniciação e a propagação da corrosão sob tensão são processos muito complexos, um processo de fratura ambientalmente assistida, ao lado de corrosão-fatiga e fragilização por hidrogênio, dependendo de vários parâmetros que são classificados em microestruturais, mecânicos e ambientais. Por causa dessa complexidade, há vários modelos que podem quantificar esse tipo de falha. Para aços inoxidáveis e ligas de níquel em reatores de água leve a alta temperatura, há diversos mecanismos que permitem expressar matematicamente os processos cinéticos de iniciação e propagação da corrosão sob tensão: modelo de fluência de Rice, modelo de deslizamento subsuperficial com ruptura do filme passivo de Ford e Andresen, modelo de oxidação interna de Scott e Le Calvar, modelo de mobilidade superficial acelerada de Galvele, modelo numérico de Rebak e Smialowska, modelos de trinca induzida por hidrogênio de Shen e Shewmon, Magnin e outros. O modelo baseado no mecanismo de mobilidade superficial acelerada, desenvolvido por José Galvele na Argentina, é um dos principais que quantificam a taxa de propagação de corrosão sob tensão em ligas recobertas com filmes de baixos pontos de fusão e com cátions como Ag⁺ (ligas de Ag-Cd) e Cu²⁺ (latão). Também é adequado para a liga de níquel Inconel 600. Neste artigo são mostrados os resultados do modelo de mobilidade superficial aplicado em corpos de prova de liga 600 ensaiados nos equipamentos de taxa de deformação lenta do Centro de Desenvolvimento da Tecnologia Nuclear - CDTN, em Belo Horizonte.

Palavras-chave: Corrosão sob tensão; Ensaio de taxa de deformação lenta; Liga inconel 600; Modelo de mobilidade superficial.

¹ Technical contribution to 67th ABM International Congress, July, 31th to August 3rd, 2012, Rio de Janeiro, RJ, Brazil.

² Post Doctoring Researcher, Nuclear Engineering Center, IPEN/CNEN, USP, São Paulo, Brazil.

³ Researcher and Professor, Nuclear Engineering Center, IPEN/CNEN-USP, São Paulo, Brazil.

⁴ Researcher and Professor, CDTN/CNEN, UFMG, Belo Horizonte, Brazil.

1 INTRODUCTION

The stress corrosion cracking (SCC) is a complicate degradation process, and depends upon many parameters.^(1,2) These ones can be classified in microstructural, mechanical and environmental.⁽³⁾

The mechanical factors are: (1) applied and residual stresses: these stresses and geometry can be summarized as stress intensity K (optionally, can be used strain and strain rate which can be also described related to stresses). The microstructural factors are: (2) grain boundary chemistry and segregation; (3) thermal treatment which can causes intragranular and intergranular metallic carbide distribution; (4) grain size and cold work or plastic deformation - the two last ones fix the yield strength: these factors can be described as A in Figure 1. The environmental factors are: (5) temperature T ; (6) activity of $[H]^+$ or pH; (7) solution or water chemistry; (8) inhibitors or pollutants in solution: these two last ones can be described as $[x]$ in Figure 1; (9) electrochemical and corrosion potentials E and E_0 ; (10) partial pressure of hydrogen which reflects on potential.⁽³⁾ This environmental cracking susceptibility can be expressed as showed in Figure 1.⁽⁴⁾

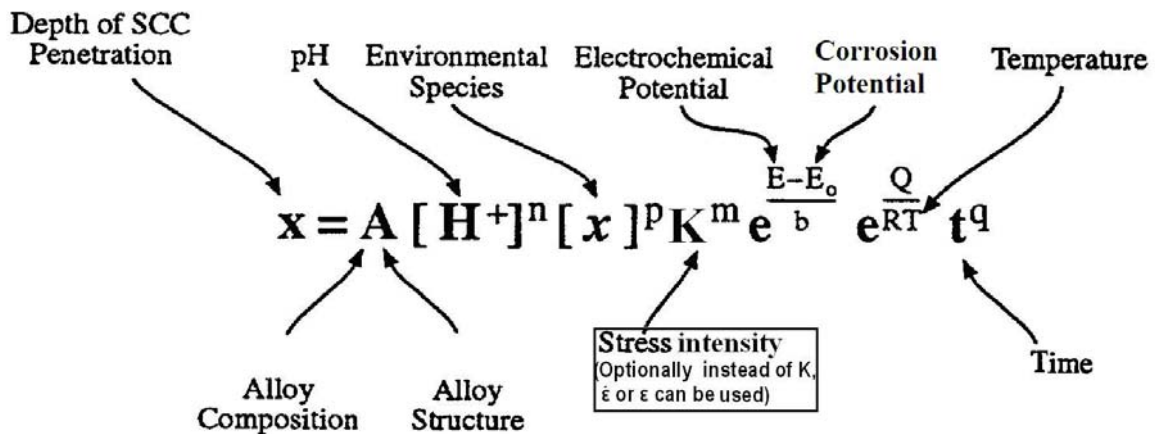


Figure 1. General phenomenological relationship for SCC process depending on many parameters; b , m , n , p , q are adjusted constants, Q the thermal activation energy, and R the universal gas constant.⁽⁴⁾

Therefore there are some models to give to SCC mechanisms a mathematic description. In this paper, one considers a SCC case in nickel Inconel alloy 600, at high temperature (280°C to 360°C) water to PWR (pressurized water nuclear reactors). For these case, the main applicable models are the slip-step dissolution and film rupture model as developed by Andresen and Ford, the internal oxidation mechanism of Scott and Le Calvar, the enhanced surface mobility mechanism of Galvele, the numerical model of Rebak and Smialowska, hydrogen induced cracking models of Shen and Shewmon, Magnin and others.⁽³⁾

The model based on enhanced surface mobility mechanism, developed by José Galvele in Argentina, is one of the main ones which quantify the crack propagation rate of stress corrosion cracking.

In this paper one aims to test the Galvele model capability to adjust the data obtained in CDTN using SSRT with alloy 600 specimens at the mentioned PWR circuit water condition.

2 THE ENHANCED SURFACE MOBILITY MODEL

The model's mechanism was formulated based on the similarities between different embrittlement occurrences and over many environmentally assisted cracking theories.

It is based on the atomic surface diffusion caused by a stress potential difference, then provoking a crack advance by the capture of vacancies by a crystalline lattice at the crack tip, due to the atoms displacement. The crack propagation rate is dependent by the atomic displacement adsorbed along the crack edges and the environment can modify the surface mobility through different diffusivity characteristics. In Figure 2, one can see a draw showing the mechanism's action: the stress gradient between the crack tip and the crack edge surface, promotes the A-B atomic displacement, introducing a vacancy at the crack tip, and advancing the crack one atomic distance. The adsorbed C atom will be transported through a new lattice site D, by surface diffusion which can vary depending to the interaction material-environment.⁽⁵⁾

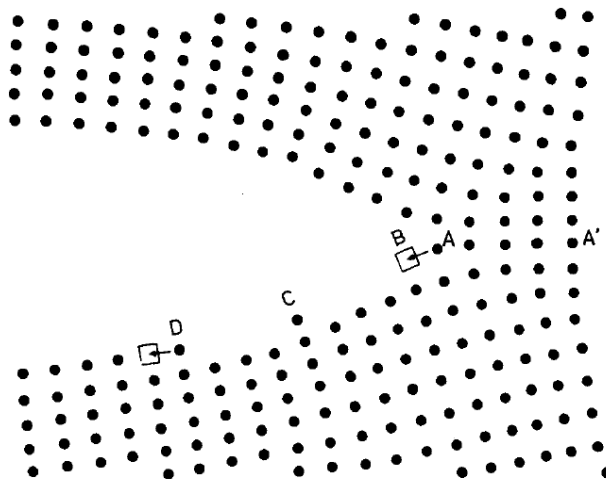


Figure 2. Schematic drawing showing the surface enhanced mobility mechanism action.⁽⁵⁾

The crack propagation rate is deduced⁽⁵⁾ as Equation 1.

$$v_{SCC} = (D_s / L) \cdot [\exp(\sigma \cdot a^3 / k \cdot T) - 1] \quad (1)$$

Where: v_{SCC} is the crack velocity [$m \cdot s^{-1}$]; D_s the surface self-diffusion coefficient [$m^2 \cdot s^{-1}$]; L , diffusion distance [m], σ , elastic surface stress at the crack tip [$N \cdot m^{-2}$]; a , the atom size [m], k , the Boltzman constant [$J \cdot K^{-1}$], T , absolute temperature [K].

The surface diffusivity D_s can be estimated by Gjostein e Rhead's correlation according Equation 2.

$$D_s = 7,4 \cdot 10^{-2} \exp - (30 \cdot T_m / R \cdot T) + 1,4 \cdot 10^{-6} \exp - (13 \cdot T_m / R \cdot T) \quad (2)$$

Where: R is the universal gas constant [$1, 987 \text{ cal/mol} \cdot K$], T_m is the melting point of the surface component formed between material and environment [K].

In Alloy 600 case, that component in contact with primary water environment, is composed by a metallic oxides mixture such as Fe_3O_4 , NiO , and Cr_2O_3 . According Galvele, if $D_s \geq 10^{-16} m^2 / s$ the melting compound causes material susceptibility to stress corrosion cracking.⁽⁵⁾

If one considers in Equation 1 the hydrogen effect through the hydrogen embrittlement mechanism, and liquid metal embrittlement in metals which don't have the hydrides formation around the crack tips, then will result the Equation 3.⁽⁵⁾

$$v_P = (D_s / L) \cdot \{ \exp [(\sigma \cdot a^3 + \alpha \cdot E_b) / k \cdot T] - 1 \} \quad (3)$$

Where: v_P is the crack propagation velocity; D_s the surface self-diffusion coefficient; L , the diffusion distance; σ , the elastic surface stress at the crack tip; a , the atom size; k , the Boltzman constant; T , the absolute temperature; α , a dimensionless function which measures the difference in degree of saturation with hydrogen of the vacancies; E_b , the binding energy for H- monovacancies in the nickel.

3 MATERIAL AND TEST METHOD

In the SSRT developed at CDTN it has been used Alloy 600 MA specimens, and test standard practice according ASTM-G-129-00. In the Tables 1 and 2 it was presented the chemical composition and the mechanical properties respectively. In the Figure 3, it is showed details of the CDTN installation.

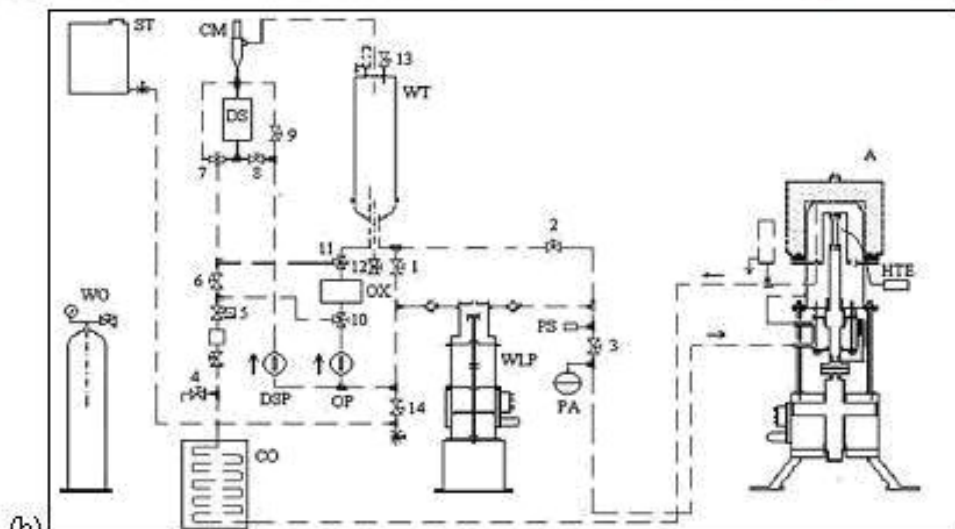
Table 1. Chemical composition of Alloy 600 MA (% weight)^(6,7)

C	Mn	P	S	Si	Ni	Cr	Co	Cu	Fe	Al	Ti	Nb
0.042	0.22	0.008	0.0002	0.18	75.05	15.61	0.10	0.03	8.81	0.08	0.20	0.20

Table 2. Mechanical Properties of Alloy 600 MA^(6,7)

Temperature (°C)	σ_Y (MPa)	σ_T (MPa)	Deformation (%)	Area Reduction (%)	Hardness HB
22	302	632	38,5	62	170
300	254	567	38,6	58	N.A.

σ_Y – yield strength; σ_T – tensile strength.



- Autoclave
- CM-Conductivity Meter
- CO-Cooler
- DS-Demineralizer Station
- OP-Oximeter Circulation Pump
- EP-Exchange Filter Circ. Pump
- HTE-High Temperature Electrode
- PA-Pressure Accumulator
- PS- Pressure Sensor
- WT-Water Tank
- ST-Service Tank
- WG-Work Gas
- WLP- Water Circulation Pump

Figure 3. (a) Photo of CDTN installation for SSRT: at center, inside the metallic structure is located the autoclave-electrode assembling for high-temperature, where are disposed the SSRT specimens; at left, the water circulation pump assembling; (b) water circuit drawing of the installation.^(6,7)

The environment composition used in the tests was a solution with deionized water containing a chemical composition similar to the environment of the primary circuit of a pressurized water reactor in operation (temperature 303°C). This solution contains 1,000 ppm to 1,200 ppm of boric acid, 2.2 ppm to 2.5 ppm of lithium hydroxide, 25 cm³ to 35 cm³ CNTP H₂/kg H₂O, and less than 5 ppb of O₂. During the tests, the pH was maintained between 6.9 and 7.4. The main results of the tests are shown in Table 3 and Figure 4.^(6,7)

Table 3. Results of semi-quantitative tests to evaluate PWSCC in Alloy 600, developed at CDTN: neutral environment (nitrogen), and primary water environment. Test strain rate of $3 \times 10^{-7} \text{ s}^{-1}$.^(6,7)

Test	SSRT 01	SSRT 02	SSRT 03
Environment	Nitrogen	Primary Water	Primary Water
Test Time (days)	21.3	20.1	20.6
Estimated Time to Initiation (h)	---	482.4	494.4
Test Velocity ($\mu\text{m/h}$)	34.1	33.0	33.0
Pressure (MPa)	2.05	10	10
Yield Strength (MPa)	275	292	265
Tensile Strength (MPa)	647	648	650
Deformation (%)	55.8	53.5	54.1
Area Reduction (%)	55.5	50.9	51
Failure Time Rate	---	0.94	0.97
Deformation Rate	---	0.96	0.97
Area Reduction Rate	---	0.92	0.92
Tenacity (kJ/m^3)	29.51	27.49	27.89

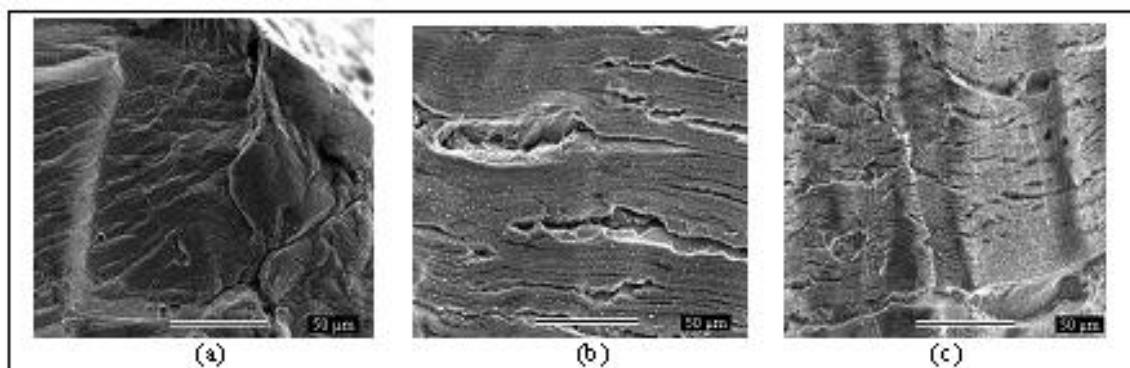


Figure 4. SEM-microfractographies, increased 500 times, showing the Alloy 600 MA specimen's lateral surfaces. The tests were realized with slow rate test ($3.0 \times 10^{-7} \text{ s}^{-1}$), at 303°C and 10 MPa. (a) SSRT 01 (N_2 -environment); (b) SSRT 02 (PW-environment); (c) SSRT 03 (PW-environment).⁽⁷⁾

4 MODELING STUDY - RESULTS AND DISCUSSION

It has been done the estimated calculation by the enhanced surface mobility model, to the CDTN tests using Alloy 600. This result was compared with the estimated calculation for the average crack propagation rate (with slow crack propagation), considering the CDTN tests: this was of $5.69 \times 10^{-11} \text{ m/s}$, corresponding to the cracks average rate at test time.⁽⁸⁾

Basically, it were used the Equations 1 to 3, to the modeling estimation. The assumed values to this calculation are as following:

- environment temperature where the PWSCC with Alloy 600 occurs:
 $T=303^\circ\text{C}$.^(6,7)
- $L=10^{-8} \text{ cm}$ for NiO – PWSCC of Alloy 600 (p. 2123 from Galvele⁽⁹⁾);
- D_s is estimated from linear interpolation between the critical values of the row 2 of Table 1 from Rebak e Szklarska-Smialowska⁽³⁾ (here reproduced as Table 4): the critical value for D_s is related to Fe_3O_4 , $D_s \geq 10^{-16} \text{ m}^2/\text{s}$.

Table 4. D_s (m^2/s) for Alloy 600 oxides⁽³⁾

Oxide	Tm (°C)	Temperature		
		290°C	330°C	350°C
NiO	1,990	5.24×10^{-18}	3.00×10^{-17}	6.60×10^{-17}
Fe ₃ O ₄	1,597	5.11×10^{-16}	2.16×10^{-15}	4.14×10^{-15}
Cr ₂ O ₃	2,435	2.97×10^{-20}	2.39×10^{-19}	6.15×10^{-19}

The interpolation results as:

$$(330-290)/(21.6 \times 10^{-16} - 5.11 \times 10^{-16}) = (303-290)/(y - 5.11 \times 10^{-16})$$

$$y = 10.4692 \times 10^{-16} m^2/s = D_{s(crit)}^{(A600CDTN)},$$

d) $\sigma = 650$ MPa;^(6,7)

e) $a = 2.5 \times 10^{-10}$ m (atom diameter value, from reference⁽³⁾);

f) $k = 1.38 \times 10^{-23}$ J/K (Boltzmann constant);

g) $T = 303^\circ C + 273.3 = 576.3$ K;

h) CPR is obtained replacing all values from (a) to (g) in Equation 1:

$$CPR = 10.4695 \times 10^{-16} / 10^{-10} \{ \exp [(650 \times (2.5 \times 10^{-10})^3 / 1.38 \times 10^{-23} \times 576.3)] - 1 \}$$

$$CPR = 1.3369 \times 10^{-11} m/s;$$

i) then, the velocity obtained by this model was about 23% from the estimated velocity using the results of the CDTN experiments: in this case, other processes should be influenced, such as anodic process, film-rupture, or the hydrogen effect;

j) one can calculate CPR' including the hydrogen effect, through Equation 3;

k) if one inputs a value for $\alpha = 1$ (p. 20 from Galvele⁽⁵⁾), that corresponds to the maximum hydrogen effect which is near the phase changing Ni/NiO;

l) Value of E_b (Ni) = 0,43 eV (p. 20 from Galvele⁽⁵⁾);

m) $CPR' = 2.5112 \times 10^{-11}$ m/s;

n) in this case, $CPR' = 5.62 \times 10^{-11}$ m/s, value near the estimated value for CDTN experiments = 5.69×10^{-11} m/s

o) but to admit this value, it's necessary to confirm if the CDTN experiments are done with the maximum hydrogen effect: according the MRP-213,⁽¹⁰⁾ this occurs in the changing of phase Ni/NiO, as shown in the Figure 5: for $T = 325^\circ C$, this peak is around the hydrogen fugacity of $10 \text{ cm}^3 \text{ H}_2/\text{kgH}_2\text{O}$. For to calculate the H_2 fugacity on the line Ni/NiO, the MRP-213 suggests the empirical Equation 4.

$$\text{H}_2 \text{ Fugacity (Ni/NiO) } [cm^3/kgH_2] = 10^{(0.0111 * T(oC) - 2.59)} \quad (4)$$

For the CDTN actual test condition, $T = 303^\circ C$, then H_2 Fugacity $_{(Ni/NiO)}^{CDTN} = 5.933 \text{ cm}^3/\text{kgH}_2$, but if tests were realized at $325^\circ C$, then H_2 Fugacity $_{(Ni/NiO)} = 10.411 \text{ cm}^3/\text{kgH}_2$, value which corresponds to the fugacity for CGR peak-value in Figure 5.

So, the CPR' – value obtained for the maximum hydrogen effect according with the enhanced surface mobility model with CDTN tests is consistent with the MRP-213 assumptions for the maximum PWSCC crack growth rate around the hydrogen fugacity of $10 \text{ cm}^3 \text{ H}_2/\text{kgH}_2\text{O}$.

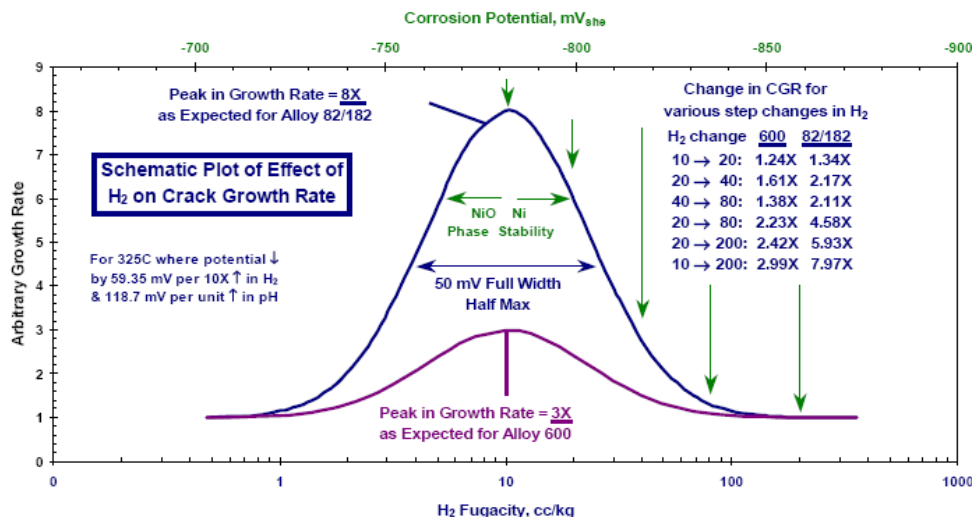


Figure 5. Variation of the arbitrary growth rate with the hydrogen fugacity, for desaturated water, according MRP-213 prediction of the hydrogen effects on PWSCC growth rate at 325°C. The peak is associated with the Ni/NiO phase boundary.⁽¹⁰⁾

5 CONCLUSIONS

The survey carried out using data from CDTN shows that this mechanism can adjust well to Alloy 600 PWSCC, if it is considered $\alpha = 1$, so that is to admit the maximum hydrogen effect. This however has not yet been experimentally proven in CDTN tests. It is also possible that the enhanced surface mobility mechanism is responsible for only a part of the crack propagation rate. Originally this mechanism was conceived and applied in alloys with low melting point and cations such as Ag⁺ (Ag-Cd alloys), and Cu²⁺ (brass), but it also adjusts well to Alloy 600.

Acknowledgment

Capes (Coordenação de Aperfeiçoamento de Pessoal de Nível Superior- Brasil) for the research fund, IPEN/CNEN-USP (Instituto de Pesquisas Energéticas e Nucleares/ Conselho Nacional de Energia Nuclear- São Paulo University – Brazil) for the research opportunity and infrastructure, and CDTN/CNEN-UFMG (Centro do Desenvolvimento da Tecnologia Nuclear/ Conselho Nacional de Energia Nuclear, Federal University of Minas Gerais – Brazil) for the experimental data availability.

By a sad coincidence, while we were working in the research which originates this paper, we learned of the death of Dr. José Rodolfo Galvele (1937-2011), held on July 31 of the past year. José Galvele will remain as one of the exponents of Materials Science in Argentina and Latin America. This paper stands as an heartfelt tribute to Galvele and is dedicated to him.

REFERENCES

- 1 FONTANA, M.G., GREENE, N.D. Corrosion Engineering. New York: McGraw-Hill, 1978.
- 2 HERTZBERG, R. W. Deformation and Fracture Mechanics of Engineering Materials, New York: John Wiley&Sons, 1989.
- 3 REBAK, R.B., SZKLARSKA-SMIALOWSKA, Z. The mechanism of stress corrosion cracking of alloy 600 in high temperature water, *Corros. Sci.*, v.38, p. 971-988, 1996.

- 4 STAEHLE, R.W. Bases for Predicting the Earliest Penetrations Due to SCC for Alloy 600 on the secondary Side of PWR Steam Generators, Argonne, Illinois: Argonne National Laboratory, 2001. (NUREG/CR-6737, ANL-01/20 RWS 151, Sept. 2001)
- 5 GALVELE, J.R. A stress corrosion cracking mechanism based on surface mobility. *Corros. Sci.*, v.27, n. 1, p. 1-33, 1987.
- 6 SCHVARTZMAN, M.M.A.M., NEVES, C.F.C., MATIAS, A., LOURENÇO, L.I. Avaliação da Susceptibilidade à Corrosão Sob Tensão do Inconel 600 MA em Ambiente de Reator Nuclear, In.: CONGRESSO ANUAL DA ABM-INTERNACIONAL, 60, Anais... Belo Horizonte: ABM, 2005. 1CD.
- 7 MATIAS, A., SCHVARTZMAN, M.M.A.M. Development of a Methodology for Evaluation of Susceptibility to Stress Corrosion Cracking in Nuclear Reactor Environment, In.: INAC 2005, Proceedings...Santos, Brazil, INAC, September 2005. 1 CD. (in Portuguese)
- 8 ALY, O.F., MATTAR NETO, M., SCHVARTZMAN, M.M.A.M. A Methodology for Modeling Stress Corrosion Cracking with an Example, In.: COBEM-Brazilian Congress of Mechanical Engineering, 21, *Proceedings*...Natal: ABCM, 24-28 Oct. 2011, 1 CD.
- 9 GALVELE, J.R. Reply to “Notes on the discussion concerning the “surface mobility mechanism” of stress corrosion cracking”, by E.M.Gutman. *Corros. Sci.*, v. 45, p. 2119-2128, 2003.
- 10 *MATERIALS RELIABILITY PROGRAM: Mitigation of PWSCC in Nickel-Base Alloys by Optimizing Hydrogen in the Primary Water (MRP-213)*. EPRI, Palo Alto, CA: 2007. 1015288. Available at:
<http://my.epri.com/portal/server.pt?space=CommunityPage&cached=true&parentname=ObjMgr&parentid=2&control=SetCommunity&CommunityID=221&PageIDqueryComId=0>
(Search for “1015288”). Accessed on April 2009.